

# Potential Utilization of Iraqi Associated Petroleum Gas as Fuel for SI Engines

Jehad A. A. Yamin<sup>a</sup>, Eiman Ali Eh Sheet<sup>b</sup>

<sup>a</sup>Mechanical Engineering Department, School of Engineering, The University of Jordan, Amman 11942, Jordan

<sup>b</sup>Energy and Renewable Energies Technology Center, University of Technology-Iraq, Baghdad 10066, Alsenaa Street, Iraq

Received October 19 2019

Accepted August 31 2020

## Abstract

An engine modelling study was conducted to investigate the relative change in performance and emissions of a 4-stroke, spark-ignition engine using Iraqi Associated Petroleum Gas as fuel. The research was done using a well-verified simulation software Diesel-RK. The data available for Ricardo E6/T variable compression ratio spark-ignition engine was used to conduct this study. The performance of the engine using associated petroleum gas was compared with those for gasoline, natural gas, and the average properties of the natural gas in Europe. The performance parameters studied were engine power, thermal efficiency, oxides of nitrogen, unburned hydrocarbon, and carbon monoxide levels. The study showed that the Iraqi associated petroleum gas could not be used "as is" if the aim is to cut down pollution. The main advantage is the absence of sulfur in the gas, which is present in the gasoline used in Iraq. There is a significant rise in NO<sub>x</sub> levels, a reduction in UHC, and also a rise in CO levels when using APG fuel. Further, there is an average reduction in engine power of about 10% with the associated gas compared with gasoline. At the same time, the only gain is the reduction in SFC and improvement in thermal efficiency with the new fuel.

© 2020 Jordan Journal of Mechanical and Industrial Engineering. All rights reserved

Keywords: Associated gas, SI engine, Methane gas, Engine emissions, Natural gas;

## 1. Introduction

Gaseous deposits that often exist in petroleum are usually called Associated Petroleum Gas (APG) or Flare gas (FG). These gaseous deposits usually consist of methane and other short-chain hydrocarbons which are considered as by-product of oil production. They are, in many cases, either flared or vented.

With reference to the data collected from satellites, the quantity of this gas that gets flared and vented annually in the world is estimated to be 140-170 billion cubic meters (BCM) (Elvidge et al., 2009, and 2013, <https://visibleearth.nasa.gov/view.php?id=83178>, Vorobev and Shchesnyak, 2019). Iraq burned approximately 30 BCM of APG in 2018 (<https://www.iea.org/reports/iraq-energy-outlook-2019>), and it is estimated according to the report that this quantity will rise to around 50 BCM.

Flaring is preferable to venting from a global warming point of view. Though this process produces Carbon Dioxide (CO<sub>2</sub>), it, however, reduces the overall potential for global warming caused by methane and other hydrocarbons. Methane that is present as deposits in petroleum is considered to be (on a 100 years time-scale) more potent than CO<sub>2</sub> (Holmes et al., 2013; Myhre et al., 2013; Boucher et al., 2009).

Though flaring helps reduce global warming gases that are flammable in nature, it, on the other hand, produces some other pollutants, such as Oxides of Nitrogen (NO<sub>x</sub>), Carbon Monoxide (CO), and Black Carbon (BC). One of the by-products of APG flaring is BC. This by-product causes climate warming, speeds up ice melting and blackens its surface, and affects the dynamism of the clouds. (Myhre et al., 2013).

It was estimated that 4% of the global BC emissions are produced by APG flaring. With an estimated amount of 230 Gg/yr, this is considered more than three times higher than spark ignition engines' vehicles global BC emissions of about 80 Gg/yr (Boucher et al., 2009, Bond et al., 2013, Stohl et al., 2013). APG can be utilized in so many ways provided they are processed in certain ways. Some ways of the utilization of APG include power generation which is sold out for certain chemical and petrochemical industries, injected in petroleum well to improve oil recovery.

Upon reviewing the literature, limited or no research is found on the use of this gas as a fuel for Spark Ignition (SI) engines. Zyryanova et al. (2013) showed a faster payback of the capital investment achieved for the power plants that used fuel made catalytic reforming of APG into Methane-hydrogen mixture compared with direct burning of APG only. They attributed this to the extended service life, extended durations of overhaul, and low rated power losses.

\* Corresponding author e-mail: yamin@ju.edu.jo

AI Gur'yanov et al. (2015) conducted a computational analysis on the effect of converting Natural Gas (NG) powered gas turbine combustion chamber to be fueled with APG. They took into their consideration the change in power density, thermal and combustion efficiencies as well as engine-out emissions. One of the significant conclusions they reported was the need to redesign the air distribution system as well as the method of fuel introduction due to the variable composition of the APG from field to field compared with methane gas.

Vazim et al. (2015) conducted an economic study on the use of APG as fuel in a small power generation unit in Tomsk Oblast. They showed increase in profitability and reduced payback period when using this type of fuel.

Using APG as fuel for SI engines resulted in a new concept of the fuel's tendency to resist knocking rises. Methane Number (MN) (Roy et al., 2019), is a new term used to indicate the fuel's ability to resist knocking (similar to Octan Number (ON) in conventional fuels).

Methane is usually given an arbitrary number of 100 (being strong resistant to knocking) while hydrogen is given the scale of zero due to its relative fast burning compared with methane. MN can be determined by the percentage of methane in the mixture of methane and hydrogen that will give the same knocking characteristics of the test fuel. Thus, a fuel with MN=90 means that this fuel has knock resistance equivalent to a mixture of 90% methane and 10% hydrogen.

APG flaring in Iraq has increased in mid-1970s. This situation continued till the Gulf War in 1992 where it reduced significantly and then rose again in 2011 to a level of 9.4 BCM of natural gas. Some known agencies estimated that around 70% of APG in Iraq is being wasted by flaring. (<https://visibleearth.nasa.gov/view.php?id=83178>).

Significant amount of research and efforts have been directed towards improving utilization of APG in Iraq and Arab countries to be used in fertilizers, power generations and other applications.

It was estimated that in 2013, 21.8 BCM of APG (out of a total of 24 Million Barrel per Day (MBD)) was flared. This amount increased in 2017, to about 25.5 BCM (out of a total of 26 MBD of crude oil produced). These figures indicate that the amount of APG being lost by flaring has increased, thus, increasing the loss in a potential source of energy. (<https://www.ecomena.org/gas-flaring-in-iraq/>).

More recently and with the energy crisis due to unrest in the region, the value of gas as a source of energy and its environmental benefits were gradually realized, and some regulations were introduced to limit gas flaring to the minimum.

Based on the above introduction, it becomes clear that APG represents a potential source of energy that must be investigated in the automobile sector. This paper discusses the relative change in spark-ignition engine emissions and performance when using Iraqi APG as fuel compared with gasoline, natural gas (NG), and pure methane.

## 2. The Study

### Mathematical modeling

This model treats the combustion chamber in a way that it consists of two distinct zones (e.g. burned and unburned) separated by the flame front. The main equations applied to

analyse those zones are the first law of thermodynamics and the continuity equation. These equations are derived with respect to crank angle ( $\theta$ ) to yield several coupled first order differential equations for pressure, volume, temperature (burned and unburned), mass, heat flux ...etc. that are applied for both zones. As for the cylinder pressure, it is usually assumed to be in uniform all through the cylinder charge. The model is also assumed to have no chemical reaction between cylinder constituents prior to combustion, and that the mixing inside the cylinder between its constituents is a perfect one.

Derivation of the equation of state with respect to  $\theta$  gives (Yamin et al., 2003):

$$\frac{dP}{d\theta} = \frac{[-(1+\frac{R}{C_v})P\frac{dV}{d\theta} - \frac{R}{C_v}\frac{dQ_{cr}}{d\theta} + \frac{R}{C_v}\frac{dQ_{hl}}{d\theta}]}{V} \quad (1)$$

$$\frac{dT}{d\theta} = T \cdot \left( \frac{1}{P} \frac{dP}{d\theta} + \frac{1}{V} \frac{dV}{d\theta} \right) \quad (2)$$

Where; "P" is the cylinder pressure (kPa), "T" is the cylinder temperature (K), " $\theta$ " is the crank angle (degree), "V" is the cylinder volume ( $m^3$ ) which is a function of crank angle rotation, "R" is the gas constant (kJ/kg-K), "C<sub>v</sub>" is the specific heat at constant volume (kJ/kg-K), "Q<sub>cr</sub>" is the total heat flux lost to crevice (or with blow-by) and "Q<sub>hl</sub>" is the total heat flux lost to coolant (kJ).

The instantaneous cylinder volume "V( $\theta$ )" measured from bottom dead center (BDC) position can be expressed using cylinder mechanism (slider crank mechanism) with certain modifications as :

$$V(\theta) = V_s \left[ \left( \frac{CR}{CR-1} \right) - \left( \frac{1-\cos(\theta)}{2} \right) + \left( \frac{CRL}{S} \right) - \frac{1}{2} \sqrt{\left( \frac{2 \cdot CRL}{S} \right)^2 - \sin^2(\theta)} \right] \quad (3)$$

Where; "CR" is the compression ratio, "CRL" is the connecting rod length (m), "S" is the stroke length (m), and "V<sub>s</sub>" is the stroke volume ( $m^3$ ).

Derivation of equation (3) with respect to  $\theta$  gives the rate of change of cylinder volume with crank angle as follows :

$$\frac{dV}{d\theta} = \frac{1}{2} V_s \sin \theta \left( \frac{\cos \theta}{\sqrt{\left( \frac{2 \cdot CRL}{S} \right)^2 - \sin^2 \theta}} - 1 \right) \quad (4)$$

This is helpful in calculating the rate of change of indicated work "W" with crank angle :

$$\frac{dW}{d\theta} = P \frac{dV}{d\theta} \quad (5)$$

Also; the heat lost during the cycle (Q<sub>hl</sub>) is used as follows :

$$\frac{dQ_{hl}}{d\theta} = \frac{h_w}{\omega} A_w(\theta) [(T - T_w)] \quad (6)$$

Where; "A<sub>w</sub>" is the cylinder wall surface area ( $m^2$ ), "T<sub>w</sub>" is the cylinder wall temperature (K) and " $\omega$ " is the angular velocity ( $s^{-1}$ ).

Woschni's (1968) formula is used for the calculation of the heat transfer coefficient (h<sub>w</sub>) from cylinder contents to walls. This is shown below in equation (7).

$$h_w = \frac{P^{0.8} v^{0.8}}{T^{0.53} D^{0.2}} \quad (7)$$

where; the value of the gas velocity v is taken to be equal to 6.18\*v<sub>m</sub> during scavenging and intake stroke (m/s); and during compression stroke it takes the value equal to



**CO Formation:**

Carbon monoxide values usually lie between the maximum and the exhaust values. For this purpose, certain multiplication factor  $CO_{FAC}$  is used in the model to obtain the most correct value. This is shown below in equation (13).

$$X_{CO} = X_{CO_{eq}} + CO_{FAC} * (X_{CO_{max}} - X_{CO_{eq}}) \quad (13)$$

Where;

$X_{CO}$  = Corrected concentration of CO.

$X_{CO_{eq}}$  = Concentration of CO at equilibrium.

$X_{CO_{max}}$  = Maximum value of CO concentration at equilibrium condition.

The fuel used for this study was the APG produced in Al-Basrah (south of Iraq) oil fields. The constituents of the fuel compared with other fuels used in this study are

presented below in Table (1) ([https://www.naesb.org/pdf2/wgq\\_bps100605w2.pdf](https://www.naesb.org/pdf2/wgq_bps100605w2.pdf), <https://www.iasj.net/iasj?func=fulltext&aId=28281>)

The engine used for the study is the Ricardo E6/T variable compression ratio engine. The engine design parameters are shown below in Table (2).

The study concentrated on simulating the engine performance and emission characteristics when running the engine on the lean side to avoid excess fuel consumption, achieve the best thermal efficiency and minimum fuel consumption, and also least pollution.

The equivalence ratio was varied in the range of 0.8 to 0.95; the engine speed range was covered 1000 to 3000 rpm, ignition timing at 15° bTDC, which is nearly best for all fuels tested.

The performance of the Iraqi Associated Gas was compared with gasoline, methane, and average data gathered for the Natural gas elsewhere. This is done for the sake of comparison. The results of the study were divided into emissions and performance comparison.

**3. Results and Discussion**

First, model verification results for gasoline are shown below in Figures (1-A and B). These figures clearly show that the model was able to follow the engine behavior trends to a reasonable degree of accuracy. The model was further tested using other types of fuels as in (Yamin et al., 2000, 2002, and 2003; Hackan et al., 2008; Yamin, 2006).

Those two figures show a comparison between the experimental results as supplied by the manufacturer in the user manual and the mathematical model. The first figure (1-A) shows the comparison with the power parameters (indicated power (IP), indicated mean effective pressure (IMEP), brake power (BP), and Brake mean effective pressure (BMEP)). The second figure shows the cylinder pressure for both cases (model and simulation). The purpose of those graphs is to check the validity of the model to predict the engine behavior. As stated above, the model was verified for different types of fuels.

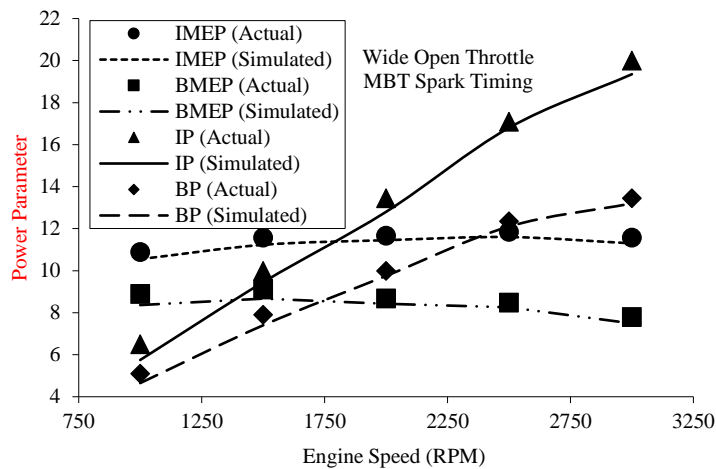


**Figure (1-A):** Comparison between experimental and model results (performance parameters)

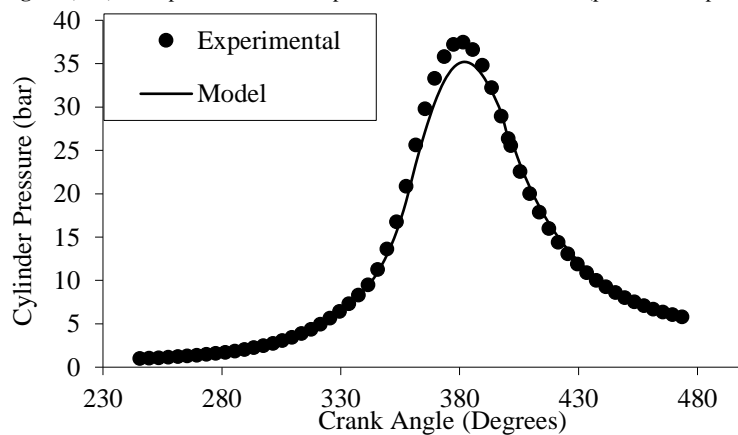


**Figure (1-B):** Comparison between experimental and model results (cylinder pressure)

**Table (1):** Fuel composition on a volume basis.

	Iraqi APG	Natural Gas	Methane	Gasoline
C1	79.5%	94.9%	100%	
C2	0.14%	2.5%		
C3	0%	0.2%		
nC4	9.24%	0.03%		
iC4	5.56%	0.03%		
nC5	0.89%	0.01%		
iC5	2.22%	0.01%		
C6	0.72%	0.01%		
H2O	0%	0%		
CO2	0%	0.7%		
N2	0%	1.6%		
O2	0%	0.02%		
H2	0%	Traces		
H2S	0%	0%		
Chemical Formula	C1.4H4.4O0.0028	C0.98H3.98	CH4	C8H18
Calorific Value (MJ/kg)	47.8	46	50	44

**Table (2):** Engine design parameters

Engine Speed (rpm)	1000-3000
Compression Ratio Range [ND]	4.5-20 (8 for this study)
Bore / Stroke (mm)	76.2/111.1
Connecting Rod Length (mm)	231.7
Crank Radius (mm)	55.5
Swept Volume (cm <sup>3</sup> )	507
Inlet Valve Open/Close (deg)	10° bTDC/36° aBDC
Exhaust Valve Open/Close (deg)	43° bBDC/8° aTDC
Maximum Valve lift Inlet/Exhaust (mm)	10.6/10.48
Tappet Clearance Inlet/Exhaust (mm)	0.152/0.203

*Engine Emissions*

The engine emissions studied were the carbon monoxide (CO), unburned hydrocarbon (HC), and oxides of nitrogen (NOx).

Before starting the discussion, let us point out the following essential points:

1. Hydrocarbon fuel burns, ideally, in two steps. First the HC molecules gets disintegrated to Hydrogen (H) and Carbon (C). Then, if the process is ideal, The C atom gets burned to CO<sub>2</sub> and that for H atom to H<sub>2</sub>O. molecules, respectively..
2. This real burning process deviates considerably from the ideal one if the fuel used is a complex (mixture of different hydrocarbons) than simple (single hydrocarbon component).
3. The more complex the combustion process is, the less effective the utilization of the fuel becomes.

In this study, the fuel used, e.g., Iraqi APG is a mixture of components that are different in nature and properties. For example, the ignition temperature in air (°C) for methane is 595, ethane 510; propane is 470, butane is 460, while gasoline has 220. Therefore, the engine needs to be modified for the new gas. Further, Octan Number (ON) of Methane, propane, and butane are higher than 100; we find that n-butane is 91, n-pentane 62, and n-hexane 25. This causes the overall mixture to behave differently during the combustion process compared with methane and other natural gas fuels.

Figure (2) shows the variation of CO with engine speeds for different equivalence ratios. It is estimated that 60% of the annual globally emitted CO gas (which is estimated to be around 2600 million tonnes) comes from industrial or human activities. The rest are from natural sources.

Those 60% emitted from human-related activities are primarily due to the incomplete combustion of the carbon atoms in the fuels. They get emitted from the exhaust system of the internal combustion engines. The most significant quantities of these type of emissions are produced as exhausts of internal or external combustion systems (e.g. engines, powerplants, incinerators ...etc.). These systems have undergone significant modifications to enhance their performance in the past few decades. ([http://www.euro.who.int/\\_data/assets/pdf\\_file/0020/123059/AQG2ndEd\\_5\\_carbonmonoxide.PDF](http://www.euro.who.int/_data/assets/pdf_file/0020/123059/AQG2ndEd_5_carbonmonoxide.PDF)).

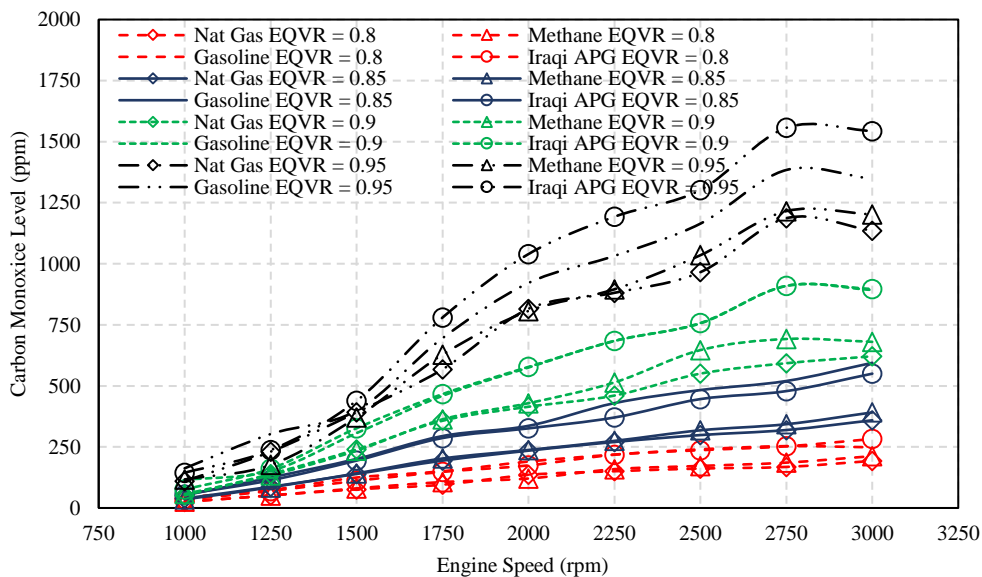


**Figure (2):** Carbon monoxide variation with engine speeds at different equivalence ratios

Generally, it is understood that the existence of CO in the exhaust of any combustion system is related to oxygen deficiency inside the combustion chamber of that system (Springer, 2012). There may be another reason for the CO to exist in the exhaust products which is the dissociation of CO<sub>2</sub> to CO and O<sub>2</sub>.

The chemical equilibrium equation for the formation of CO represented by the water gas equation as shown below :

$$\text{CO} + \text{H}_2\text{O} \rightarrow \text{H}_2 + \text{CO}_2$$

At the peak value of flame temperatures, this equilibrium produces greater amounts of CO compared to CO<sub>2</sub>. This situation occurs even if the Air/Fuel ratio used is lean. This scenario is completely altered as the products of combustion temperature falls below the peak value. This is the reason behind the less quantities of CO appearing in the exhaust when using lean or stoichiometric Air/Fuel mixtures.

For rich Air/Fuel mixtures, oxygen deficiency is the prime cause for the appearance of CO in the relatively cooler exhaust products.

As shown in Figure (3), the lower exhaust product temperature for methane and natural gas can be the reason for their lower CO levels. Further, this also explains the lower CO levels for APG at lower speeds and lower equivalence ratios.

Further, CO emissions increase with an engine speed for all fuels. This is expected to be the result of a reduction in the amount of air induced as the engine speed increases.

For all fuels, CO levels increase with the equivalence ratio. This is (as stated earlier) due to the incomplete combustion of the fuel carbonaceous contents which, due to oxygen deficiency) are partially burned.

Further, the performance of the Iraqi APG was better than gasoline for low equivalence ratios (0.8 and 0.85) for low and medium speeds. There was a maximum reduction of 20% at low speed, and the least reduction was 1.6% at 2000 rpm. At higher speeds, the performance got worsened compared with all other fuels. The increment in CO reached 13% at 3000 rpm. This is compared with other gaseous fuels, has the highest C/H ratio. Hence, higher number of carbon atoms is burned. Further, the amount of air admitted at higher gets reduced with engine speed. Therefore, the performance worsened with higher equivalence ratios and engine speeds.

Another trend shown in the figure is the advantage of using methane as fuel. For all engine speeds and

equivalence ratios, methane and natural gas produced the least CO emissions. This is due to the less carbon content of either fuels (or C/H ratio) compared with gasoline and APG. Further, those two types of fuels require less amount of air compared with gasoline and APH for complete combustion, which is already available. Similar results are shown in this review study by Singh et al. (2019).

Figure (4) shows the variation of HC with engine speeds for different equivalence ratios. Generally, HC molecules that are emitted in the exhaust are mainly unburned fuel that were deprived from getting burnt due to "flame quenching" phenomenon.

UHC can be formed due to several sources. Some of these sources are listed below :

1. Flame quenching near the cold surfaces.
2. The inability of the flame to reach certain crevices where some fuel-air mixture might exist.
3. Quenching within the bulk gas-phase due to extreme Air/Fuel conditions.
4. Fuel that gets absorbed by the lubricant during compression and later on it gets desorped as the cylinder pressure drops during exhaust process. This is known to be one of the significant phenomena.

Another theory describing the formation of HC is the crevice theory. It assumes that, especially during compression and combustion strokes, the fuel can penetrate through certain areas in the engine cylinder where the flame cannot reach (quenching distance). This part of the fuel is then gets released when the pressure drops during the expansion stroke. Some of them get burned during the after-burn process while the majority are expelled with the exhaust.

Several researchers (Lakshminarayanan et al., 2010) reported that quenching layers do exist inside the cylinder. They also showed that UHC emissions are propotional to these layers. Others reported these quench masses of the mixture are mixed with the burned mass and then get oxidized inside the cylinder during the expansion and exhaust strokes. It was estimated that less than 10% of the emitted HC was due to the wall quenching. Others attributed the HC emission due to the unburned fuel adsorption/desorption processes by lubricating oil films.

As shown in the figure below, the accelerated decrease in HC emission will be due to the reduced engine cycle time. This allows for lower absorption and desorption to occur.

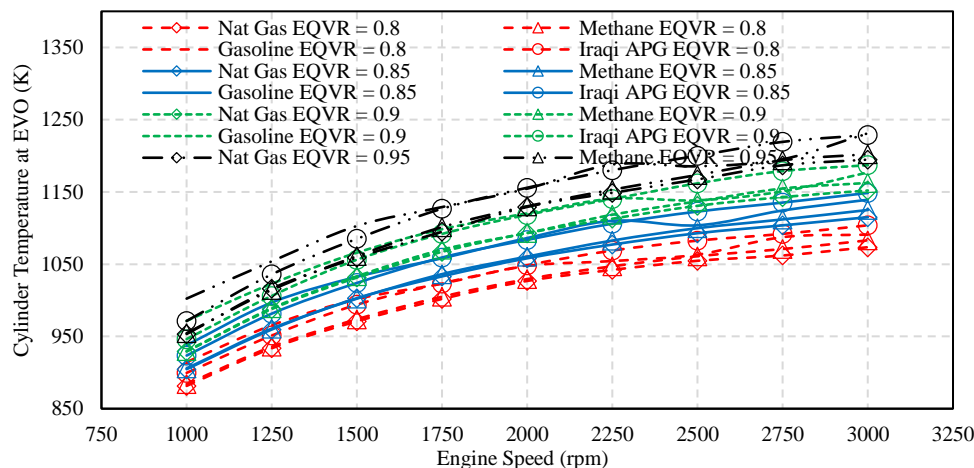


Figure (3): Exhaust temperature variation with engine speed at different equivalence ratios

With the increase in cylinder temperature at higher engine speeds, the thickness of the oil film at the wall decreases (due to reduced viscosity). This results in less amount of the unburned fuel to be absorbed by the oil film.

Henry (Lakshminarayanan et al., 2010) defined a new constant by dividing the partial pressure of the fuel vapor ( $P_{fs}$ ) in the gas phase just at the surface of the oil film to the mole fraction of the fuel dissolved in the oil film ( $n_{fl}$ ). This constant was found to increase with engine speeds and cylinder temperatures.

Another reason for the reduction of HC with engine speed is the higher exhaust temperature. This decreases the desorbed HC mass fraction (ppm) emitted due to increased wall temperature and the increased post desorption oxidation due to higher burned gas temperatures with increasing engine speed.

Further, increasing equivalence ratio ( $\Phi$ ) increases the concentration of fuel vapor in the cylinder. This will make

more of the fuel vapor to be absorbed and later on desorbed by the oil film. This phenomenon will also increase with cylinder pressure. Higher cylinder pressure will also increase the amount of mixture that will enter the crevices e.g. between rings, piston and cylinder clearance, valve and head ...etc. These places are considered as quenching distances for the flame where it cannot penetrate, hence, UHC levels will increase. This situation will be further aggravated if both the cylinder pressure and the mixture strength are increased.

Based on this, the Iraqi APG performs better than other gaseous fuels since it produces higher cylinder temperature and pressure during the cycle.

Figure (5) shows the variation of NOx emissions with engine speeds for different equivalence ratios.

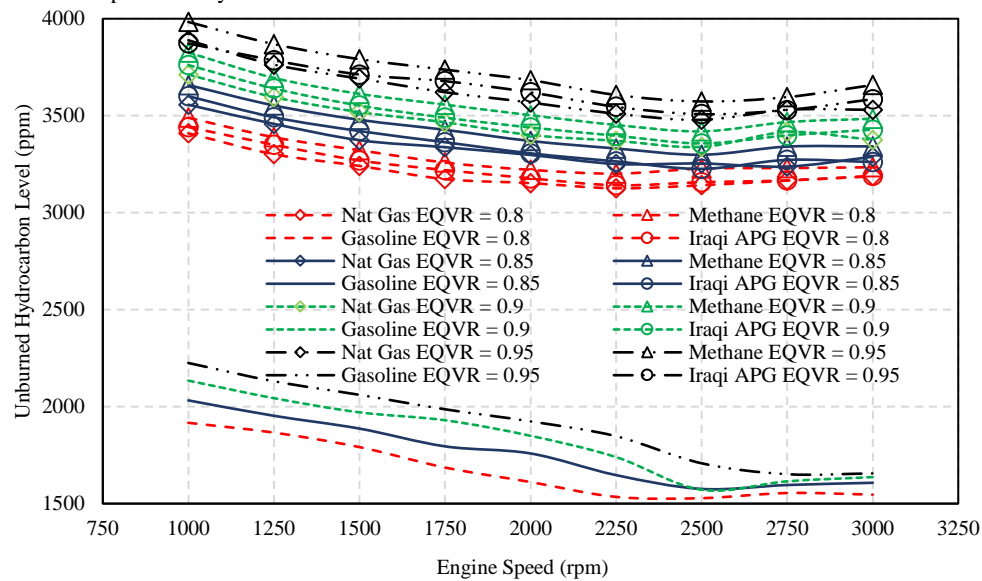


Figure (4): Hydrocarbon variation with engine speed at different equivalence ratios

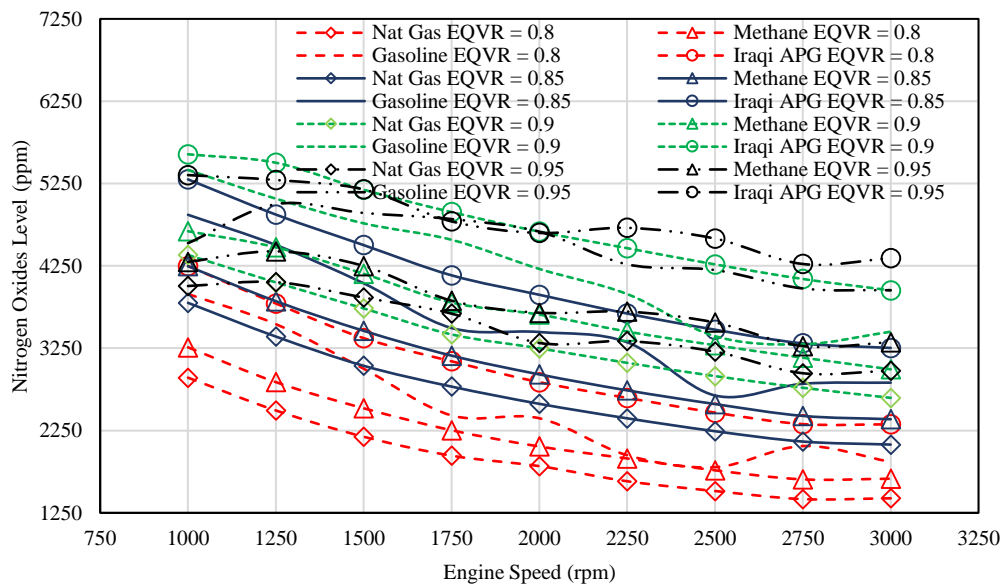


Figure (5): Oxides of nitrogen variation with engine speed at different equivalence ratios

NOx molecules in the exhaust are products of a high cylinder temperature that causes some secondary reactions that results from the disassociation of the nitrogen that enters the cylinder with atmospheric air. Some of this nitrogen also gets burned to form nitric oxide (NO), this NO is later converted to other nitrogen oxides, such as nitrogen dioxide (NO2). NOx formation depends on several factors, including cylinder temperature, oxygen availability, residence time (combustion duration), and A/F ratio.

Contrary to the behavior of CO, NOx emissions decrease with engine speed. This is clear for all fuels. The reduction in oxygen concentration and combustion duration are the primary reasons for this behavior. It is also noticed that NOx emissions are maximum for an equivalence ratio of 0.9.

As for the APG, NOx emissions are higher than others due to higher calorific value, which results in higher cylinder temperature and pressure, as shown in Figure (6).

Therefore, to conclude this section, based on the above discussion, the Iraqi association gas cannot be used "as is" if the aim is to cut down pollution. The main advantage is the absence of sulfur in the gas, which is present in the gasoline used in Iraq.

Further gas processing is needed to reduce the constituent and make it more uniform. The higher carbon components must be reduced to the least. Some studies (Lakshminarayanan et al., 2010 and Porpatham et al., 2012, Ayandotun et al., 2012) showed that the presence of CO2 in the mixture up to a certain level is helpful to cut down the NOx emissions.

On the other hand, the the higher the concentration of CO2 in the fuel mixture, the lower the heating value of this fuel mixture. This reduction in the heating value and the increase in its specific heat capacity as well reduces the flame velocity of the burned mixture and thus adversely affects the engine performance (Porpatham et al., 2012).

Engine Performance

From the engine performance point of view, brake power (Figure (7)), brake thermal efficiency (Figure (8)), volumetric efficiency (Figure (9)), and brake specific fuel consumption (BSFC) (Figure (10)).

These figures show that the power developed by the associated gas is 12% less than that for gasoline. Other fuels showed a reduction of 15% or more compared with gasoline. This is clear for all equivalence ratios studied.

Heywood (1989) developed an equation correlating engine performance parameters to power as shown below :

$$Power = \rho_{ai} A_p S \eta_{th} \eta_{vol} Q_{HV} \left(\frac{F}{A}\right) \left(\frac{N}{60}\right) \left(\frac{n_c}{n_r}\right) \quad (16)$$

where, "ρ<sub>ai</sub>" is the air density at inlet conditions, "A<sub>p</sub>" is the piston area (m<sup>2</sup>), "S" is the stroke length (m), "η<sub>th</sub>" is the indicated thermal efficiency, "η<sub>vol</sub>" is the volumetric efficiency, "Q<sub>HV</sub>" is the fuel's heating value (kJ/kg), "(F/A)" is the fuel-air ratio, "N" is the engine speed (rev/min), "n<sub>c</sub>" is the number of cylinders, "n<sub>r</sub>" is the number of stroke rotations needed to complete one cycle.

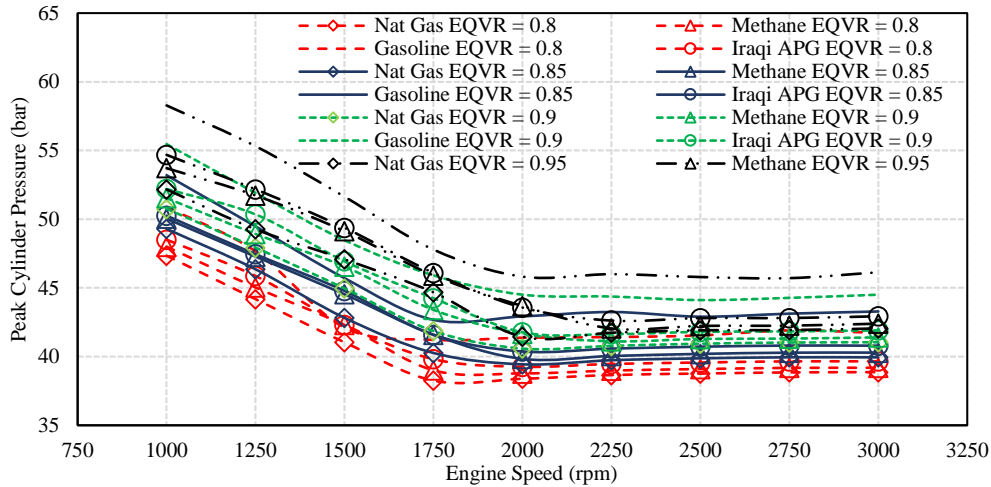


Figure (6): Peak cylinder pressure variation with engine speed at different equivalence ratios

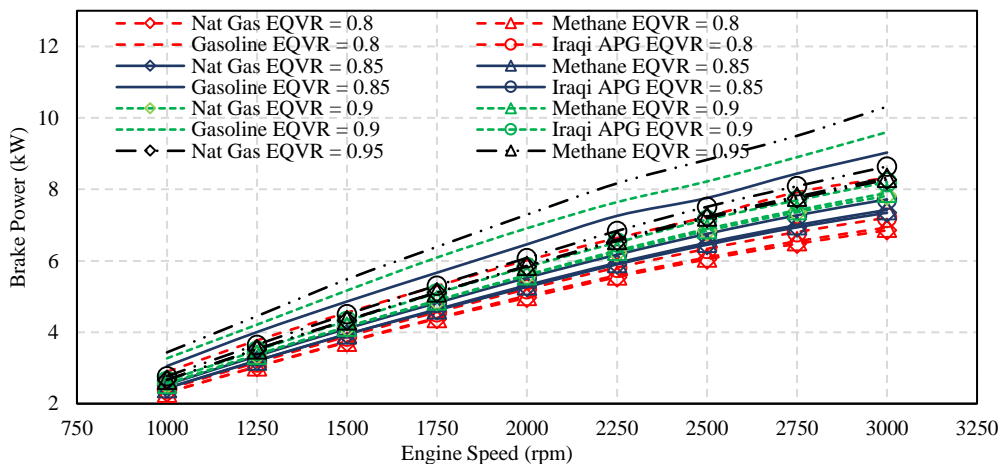


Figure (7): Brake power variation with engine speed at different equivalence ratios

As the above equations suggest, higher power can be achieved by increasing the engine displacement, engine speed, thermal efficiency, volumetric efficiency, or using fuel with higher calorific value keeping other parameters the same.

In this study, the engine dimensions were kept constant (i.e.  $\rho_{a_i} A_p S$  and  $\left(\frac{n_c}{n}\right)$ ). For each engine speed (N), the fuel equivalence ratio ( $\Phi$ ) was varied between 0.8 and 0.95. The other controlling parameters for the power (based on equation 16) will be volumetric and thermal efficiencies and calorific values.

Figure (8) shows the brake thermal efficiency for all fuels at the test conditions. It is clearly shown that the engine's thermal efficiency increases linearly for all values of  $\Phi$  from leanest till near stoichiometric. This is thought to be the result of lower cylinder temperature (compared with near stoichiometric to 10% rich mixtures) and less amount of complex components like  $CO_2$  and  $H_2O$  that are formed in the cylinder which increase the thermal capacity of the products of combustion. This, in turn, increases the amount of sensible heat resulting from converting of the fuel's chemical energy to thermal energy near top dead center. Subsequently, larger fraction of the fuel's energy is utilized to develop work inside the cylinder during expansion, and hence, less will be the amount wasted with exhaust.

This figure also shows that for all equivalence ratios, gasoline showed best results followed by APG. Thermal efficiency is also linked to the calorific value of the fuel as shown in equation (17) (Heywood, 1989):

$$\eta_{th} = \frac{Power}{\dot{m}_f Q_{cv} \eta_c} \quad (17)$$

Referring to Table (1), the calorific value of methane is the highest with 20% higher than that for gasoline. APG has

a higher calorific value than other fuels (10% greater than gasoline). However, the oxygen availability with gasoline fuel (shown in figure (9)) helped improve the combustion efficiency ( $\eta_c$ ) and hence improve thermal efficiency. This availability is also higher for APG compared with methane and natural gas. Therefore, the thermal efficiency of APG is higher than methane and natural gas. The reduction in the thermal efficiency for the methane and natural gas is of the order of 8-9%, while that for APG is 6-7% compared with gasoline.

One reason can be thought of is the latent heat of evaporation of gasoline. During evaporation, gasoline tends to cool down the engine and inlet manifold, hence increase the amount of air admitted to the engine (represented by volumetric efficiency) and, therefore, better combustion compared with gaseous fuels. Figure (9) suggests a 12-13% reduction in volumetric efficiency for methane and natural gas fuels compared with gasoline against a 9-10% reduction for APG.

The higher amount of air that the engine admits to the engine due to the cooling effect of liquid fuel being evaporated provides more oxygen for combustion and hence better combustion. Figure (9) shows the clear advantage of liquid fuel over gaseous fuel (unless the engine design is altered).

Therefore, there is quite a direct correlation between the change in thermal and volumetric efficiencies with engine power (keeping other parameters constant).

From a specific fuel consumption point of view, there is an apparent 2-3% reduction when using associated gas compared with other gaseous fuels. This is shown in Figure (10). Two factors affecting such behavior, i.e., the power developed and calorific value of the fuel.

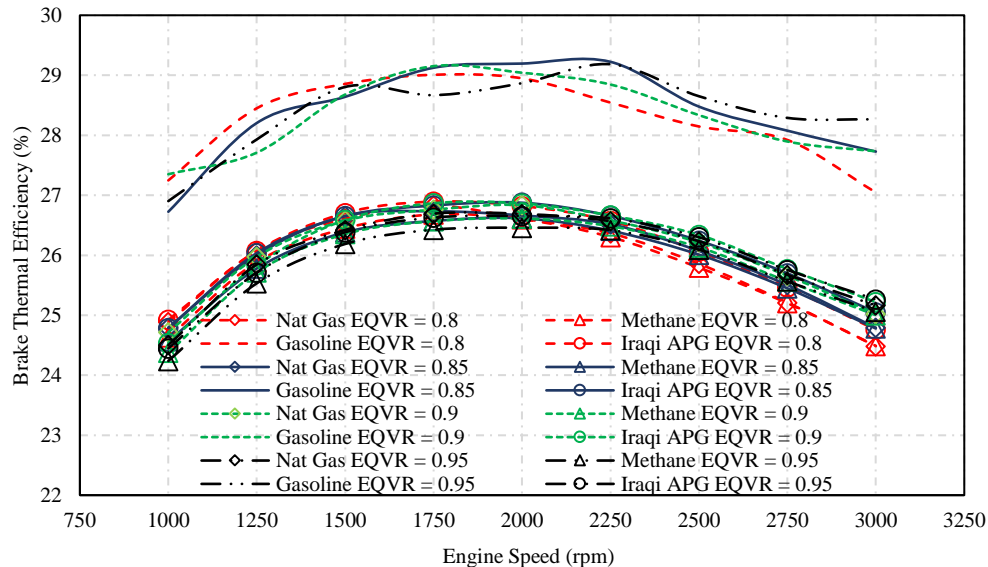


Figure (8): Brake thermal efficiency variation with engine speed at different equivalence ratios

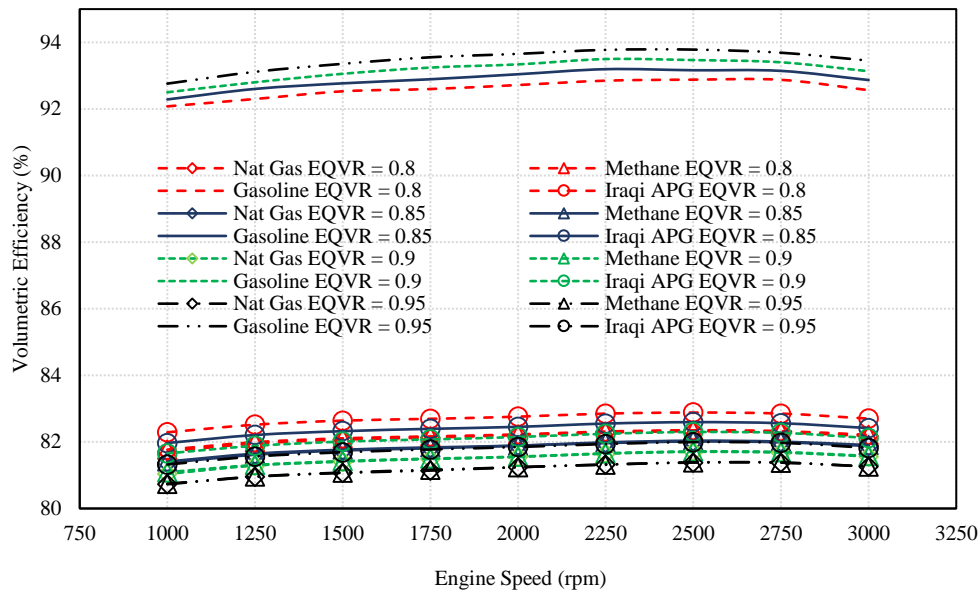


Figure (9): Volumetric efficiency variation with engine speed at different equivalence ratios

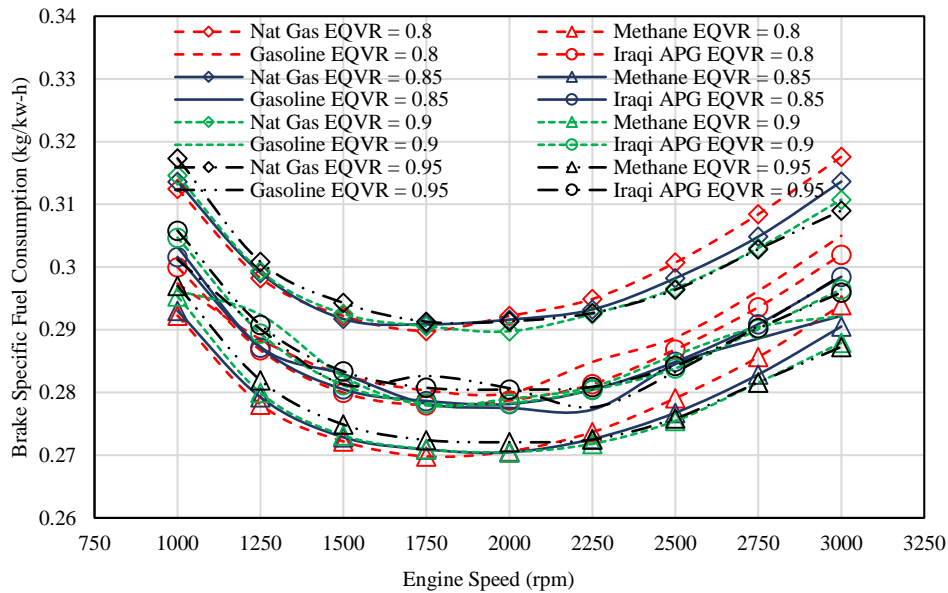


Figure (10): Brake SFC variation with engine speed for different equivalence ratios

To conclude this part, there is an average reduction in engine power of about 10% with the associated gas compared with gasoline, while the only gain is the reduction in SFC of the fuel.

4. Conclusion

A simulation study was conducted to study the performance of the SI engine using Iraqi associated gas. The study showed that the Iraqi APG needs processing before use as fuel for Si engines if the aim is to cut down pollution. The main advantage is the absence of sulfur in the gas, which is present in the gasoline used in Iraq. Further, there is an average reduction in engine power of about 10% with APG compared with gasoline, while the only gain is the reduction in SFC of the fuel.

References

- [1] Annand, W.J.D., 1974. First Paper: Effects of Simplifying Kinetic Assumptions in Calculating Nitric Oxide Formation in Spark-Ignition Engines. *Proceedings of the Institution of Mechanical Engineers*, 188(1), pp.431-436. [https://doi.org/10.1243/PIME\\_PROC\\_1974\\_188\\_049\\_02](https://doi.org/10.1243/PIME_PROC_1974_188_049_02)
- [2] Ayandotun B. Wasii, Abd. Rashid Abd. Aziz and Morgan R. Heikal, 2012. The Effect of Carbon Dioxide Content-natural Gas on the Performance Characteristics of Engines: A Review. *Journal of Applied Sciences*, 12: 2346-2350. DOI: 10.3923/jas.2012.2346.2350
- [3] Bond, T.C., Doherty, S.J., Fahey, D.W., Forster, P.M., Bernsten, T., DeAngelo, B.J., Flanner, M.G., Ghan, S., Kärcher, B., Koch, D. and Kinne, S., 2013. Bounding the role of black carbon in the climate system: A scientific assessment. *Journal of Geophysical Research: Atmospheres*, 118(11), pp.5380-5552. DOI:10.1002/jgrd.50171.
- [4] Boucher, O., Friedlingstein, P., Collins, B. and Shine, K.P., 2009. The indirect global warming potential and global temperature change potential due to methane oxidation.

- Environmental Research Letters*, 4(4), p.044007. <https://doi.org/10.1088/1748-9326/4/4/044007>
- [5] Daneshyar, H., and Watfa, M., 1974. Second Paper: Predicting Nitric Oxide and Carbon Monoxide Concentrations in Spark-Ignition Engines. *Proceedings of the Institution of Mechanical Engineers*, 188(1), pp.437-445. [https://doi.org/10.1243/PIME\\_PROC\\_1974\\_188\\_050\\_02](https://doi.org/10.1243/PIME_PROC_1974_188_050_02)
- [6] Elvidge, C., Zhizhin, M., Hsu, F.C., and Baugh, K., 2013. VIIRS Nightfire: Satellite pyrometry at night. *Remote Sensing*, 5(9), pp.4423-4449. <https://doi.org/10.3390/rs5094423>
- [7] Elvidge, C., Ziskin, D., Baugh, K., Tuttle, B., Ghosh, T., Pack, D., Erwin, E., and Zhizhin, M., 2009. A fifteen-year record of global natural gas flaring derived from satellite data. *Energies*, 2(3), pp.595-622. <https://doi.org/10.3390/en20300595>
- [8] Gatowski, J.A., Balles, E.N., Chun, K.M., Nelson, F.E., Ekchian, J.A. and Heywood, J.B., 1984. Heat release analysis of engine pressure data. SAE transactions, pp.961-977.
- [9] Gur'yanov, A.I., Evdokimov, O.A., Piralishvili, S.A., Veretennikov, S.V., Kirichenko, R.E., and Ievlev, D.G., 2015. Analysis of the gas turbine engine combustion chamber conversion to associated petroleum gas and oil. *Russian Aeronautics (Iz VUZ)*, 58(2), pp.205-209.
- [10] Heywood, J. B., 1989, *Internal Combustion Engine Fundamentals*. McGraw Hill, New York.
- [11] Holmes, C.D., Prather, M.J., Søvde, O.A., and Myhre, G., 2013. Future methane, hydroxyl, and their uncertainties: key climate and emission parameters for future predictions. *Atmospheric Chemistry and Physics*, 13(1), pp.285-302. DOI:10.5194/acp-13-285-2013
- [12] [http://www.euro.who.int/\\_data/assets/pdf\\_file/0020/123059/AQG2ndEd\\_5\\_carbonmonoxide.PDF](http://www.euro.who.int/_data/assets/pdf_file/0020/123059/AQG2ndEd_5_carbonmonoxide.PDF)
- [13] <https://visibleearth.nasa.gov/view.php?id=83178>
- [14] <https://www.iasj.net/iasj?func=fulltext&aId=28281>
- [15] [https://www.naesb.org/pdf2/wgq\\_bps100605w2.pdf](https://www.naesb.org/pdf2/wgq_bps100605w2.pdf)
- [16] Lakshminarayanan, P. A., and Yoghesh V. Aghav. *Modelling diesel combustion*. Springer Science & Business Media, 2010.
- [17] Myhre, G.; Shindell, D.; Brèon, F.; Collins, W.; Fuglestedt, J.; Huang, J.; Koch, D.; Lamarque, J.; Lee, D.; Mendoza, B.; Nakajima, T.; Robock, A.; Stephens, G.; Takemura, T.; Zhang, H., 2013, *Anthropogenic and Natural Radiative Forcing*. In: *Climate Change 2013: The Physical Science Basis. Contribution of Working Group I to the Fifth Assessment Report of the Intergovernmental Panel on Climate Change*. Cambridge University Press, Cambridge, United Kingdom and New York, NY, USA.
- [18] Porpatham, E., Ramesh, A., and Nagalingam, B., 2012. Effect of compression ratio on the performance and combustion of a biogas fuelled spark ignition engine. *Fuel*, 95, pp.247-256. <https://doi.org/10.1016/j.fuel.2011.10.059>
- [19] Roy, P.S., Ryu, C., Dong, S.K. and Park, C.S., 2019. Development of a natural gas Methane Number prediction model. *Fuel*, 246, pp.204-211.
- [20] Singh, A.P., Sharma, Y.C., Mustafi, N.N. and Agarwal, A.K., 2019. *Alternative Fuels and Their Utilization Strategies in Internal Combustion Engines*. Springer.
- [21] Springer, G. ed., 2012. *Engine emissions: pollutant formation and measurement*. Springer Science & Business Media.
- [22] Stohl, A., Klimont, Z., Eckhardt, S., Kupiainen, K., Shevchenko, V.P., Kopeikin, V.M. and Novigatsky, A.N., 2013. Black carbon in the Arctic: the underestimated role of gas flaring and residential combustion emissions. *Atmospheric Chemistry and Physics*, 13(17), pp.8833-8855. <https://doi.org/10.5194/acp-13-8833-2013>
- [23] Vazim, A., Romanyuk, V., Ahmadeev, K., and Matveenko, I., 2015. Associated petroleum gas utilization in Tomsk Oblast: energy efficiency and tax advantages. In *IOP Conference Series: Earth and Environmental Science (Vol. 27, No. 1, p. 012078)*. IOP Publishing.
- [24] Vorobev, A. and Shchesnyak, E., 2019, September. Associated Petroleum Gas Flaring: The Problem and Possible Solution. In *International Congress on Applied Mineralogy (pp. 227-230)*. Springer, Cham.
- [25] Winterbone, D., and Turan, A., 2015. *Advanced thermodynamics for engineers*. Butterworth-Heinemann.
- [26] Woschni, G., 1968. A universally applicable equation for the instantaneous heat transfer coefficient in the internal combustion engine. SAE transactions, pp.3065-3083.
- [27] Yamin, J.A., Gupta, H.N., Bansal, B.B. and Srivastava, O.N., 2000. Effect of combustion duration on the performance and emission characteristics of a spark-ignition engine using hydrogen as a fuel. *International Journal of Hydrogen Energy*, 25(6), pp.581-589.
- [28] Yamin, J.A., and Badran, O.O., 2002. Analytical study to minimise the heat losses from a propane-powered 4-stroke spark-ignition engine. *Renewable energy*, 27(3), pp.463-478.
- [29] Yamin, J.A., Gupta, H.N., and Bansal, B.B., 2003. The effect of combustion duration on the performance and emission characteristics of propane-fueled 4-stroke si engines. *Emirates Journal for Engineering Research*, 8(1), pp.1-14.
- [30] Yamin, J.A., 2006. Comparative study using hydrogen and gasoline as fuels: Combustion duration effect. *International journal of energy research*, 30(14), pp.1175-1187.
- [31] Zyryanova, M.M., Snytnikov, P.V., Amosov, Y.I., Belyaev, V.D., Kireenkov, V.V., Kuzin, N.A., Vernikovskaya, M.V., Kirillov, V.A. and Sobyenin, V.A., 2013. Upgrading of associated petroleum gas into methane-rich gas for power plant feeding applications. Technological and economic benefits. *Fuel*, 108, pp.282-291.